

Structure–Reactivity Relationship in Ketones + OH Reactions: A Quantum Mechanical and TST Approach

J. Raúl Alvarez-Idaboy,* Armando Cruz-Torres, Annia Galano, and Ma. Esther Ruiz-Santoyo

Instituto Mexicano del Petróleo, Eje Central Lázaro Cárdenas 152, 007730, México D. F., México

Received: September 18, 2003; In Final Form: January 30, 2004

CCSD(T)//BHandHLYP/6-311G(d,p) calculations have been performed to study the OH hydrogen abstraction reaction from three characteristic ketones. A previously proposed complex mechanism, involving the formation of a stable prereactive complex, is confirmed for some channels. The temperature dependence of the rate coefficients (k) is studied for all significant reaction channels over the temperature range 290–500 K, using conventional transition state theory. A good agreement between calculated and experimental k at 298 K has been obtained. The rate coefficient for the formation of the beta radical in 2-pentanone is found to be significantly larger than those of the competing channels. The explanation for this behavior, previously attributed only to the structure of the reactant complex, was found to be also a consequence of the lowering of the reaction barrier due to the presence of a hydrogen-bond-like interaction in the transition state.

Introduction

Volatile organic compounds (VOCs) are emitted into the atmosphere from a wide variety of anthropogenic and biogenic sources. They can also be formed in situ by transformations of directly emitted precursor compounds. The VOCs + OH radical reactions determine to a considerable extent the decomposition of chemical pollutants, and the rate constants (k) for these reactions are taken as a measure of the degradation time of VOCs in the atmosphere.

Ketones are among the most common pollutants: they are widely used in industry (paints, synthetic resins, etc.), and they are volatile enough to escape into the atmosphere. The conjunction of these factors is responsible for the relatively high concentration of ketones in the troposphere. Butanone, for example, is rated among the top 10 chemicals for on- and off-site releases in the EPA's 1999 Toxics Release Inventory (TRI), with more than 40 million lb released per year.¹ Global sources of ketones are secondary formation from atmospheric oxidation of precursor hydrocarbons (51%), direct emission from biomass burning (26%), and primary anthropogenic emission. Removal of propanone happens by photolysis (64%), by reaction with OH (24%), and by deposition (12%). Propanone photolysis produces the PAN precursor CH₃CO, which has been estimated to be responsible for about 50% of PAN. The average lifetime of propanone is about 16 days.² All these facts make the understanding of ketones gas-phase reactions relevant to tropospheric chemistry.

The experimental evidence^{3–11} suggests that ketones react with OH radicals via a hydrogen abstraction mechanism, leading to a water molecule and a new radical. Nevertheless, there is a peculiarity in the ketones + OH reactions: hydrogen atoms attached to carbon atoms in a beta position to the keto group are the most likely ones to be abstracted.^{3–7,11} However, if this beta carbon is a primary carbon, its contribution to the total reaction is much less important. The contribution is about 66%¹² to 67%¹³ for secondary beta carbons, while it is only about

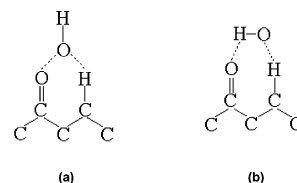


Figure 1. Reactive complex structure proposed in the literature: (a) ref 3, (b) ref 9.

11%¹² to 17%¹³ for primary ones. To explain the large contribution of the beta abstractions, Wallington and Kurylo⁴ have proposed a complex mechanism that involves the formation of a short-lived six-member ring complex. In this complex, the oxygen atom in OH radical interacts simultaneously with the oxygen atom in the keto group and with the hydrogen atom in the beta carbon (Figure 1a). Alternatively, a seven-member ring complex involving both atoms of the hydroxyl radical (Figure 1b) has been proposed by Klamt.¹³

Some experimental work has been carried out to study reactant complexes involving the OH radical.^{14,15} In addition, the role of hydrogen-bonded intermediate in bimolecular reactions of the hydroxyl radical has been recently reviewed,^{16,17} and it has been established that the presence of an attractive well in the entrance channel of a potential energy surface can influence the dynamics, and hence the course, of the reaction. The existence of a prereactive complex can be detected if the reaction presents a negative temperature dependence, which is to be expected when there is an attractive encounter between reactants. Another general feature of reactions involving this kind of intermediate is that the potential barrier separating the complex from the products should be neither too high above the energies of the reactants nor too wide so as to prevent tunneling through it. The presence of reactant complexes in OH reactions has also been studied theoretically,^{18–22} and kinetic parameters have been obtained for the complex mechanism, with results showing an excellent agreement with the experimental values.

* Corresponding author: e-mail jidaboy@imp.mx.

A recent investigation, using Carr–Parinello molecular dynamics, has been performed for the 3-hexanone + OH radical reaction.²³ At low energies the authors obtained a reaction mechanism that involves the formation of a hydrogen bond between the carbonyl group and the radical, which corresponds to the seven-member ring proposed in ref 13. It is concluded that this interaction kinetically favors the reaction at the beta position, explaining the enhanced reactivity of this site. The authors also conclude that the six-member complex proposed in ref 4 is not relevant for this reaction.

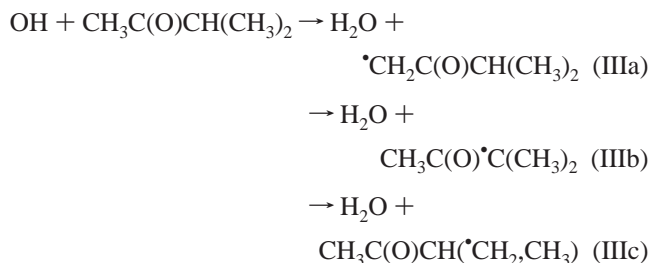
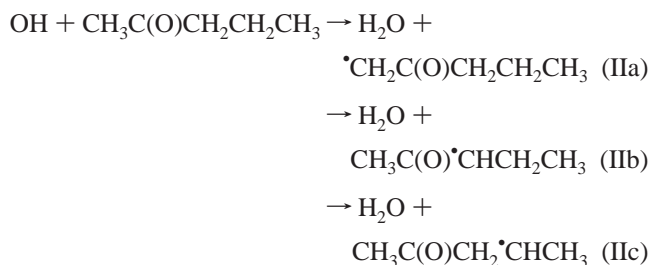
The findings in ref 23 help to understand ketones reactivity, but even though the weakly bound complexes could play a relevant role in the VOCs reactivity when they react with the OH radical, the transition states (TS) have the main role in the kinetics of these reactions. If the hydrogen-bond-like interaction is present in the TS structure, it would cause a decrease in the activation energy. The role of the prereactive complex (PRC) in the rate constant would be to favor the TS closest to the PRC geometry and to increase the tunneling effect, since the barrier from PRC is larger than the net reaction barrier. On the other hand, even though the proposed complex formation can be thought as caused by two weak attractive interactions, actually it is formed by a relatively strong hydrogen bond between the H in the OH radical and the O in the ketone and a very weak interaction between the O in the OH radical and a hydrogen in the beta site of ketones. This weakness causes the potential energy surface (PES) to be very flat for the coordinates involved in the interaction. Consequently, the oxygen in the OH also can interact with any other H in the ketone, as long as the hydrogen bond between the H in the OH radical and the O in the ketone exists. According to that, the presence of the weakly bonded complex, first proposed by Wallington and Kurylo,⁴ is necessary but not enough to explain the high reactivity of the beta sites in ketones. This kind of complex increases the reactivity of any site connecting a PRC with a transition state, not exclusively the beta sites. As far as we know, there is no published work about the possible transition structures, neither have any structural or energetic comparisons been made between the beta TS and those at sites that do not allow for a hydrogen bond interaction.

On the other hand, Cox et al.²⁴ observed acetaldehyde as a product of the OH radical reaction with butanone, with a formation yield of 0.62 ± 0.02 . Acetaldehyde is expected to arise from butanone after H atom abstraction from the alpha position ($-\text{CH}_2-$ group), and hence the fraction of the overall OH radical reaction with butanone should proceed via alpha abstraction instead of beta, according to their results. The contradiction between these results and the previously discussed ones is only apparent because the only beta H atoms present in butanone are linked to a primary carbon.

In addition significant discrepancies of 20–35%, which are not systematically high or low, have been reported⁶ between the absolute⁴ and relative rate constants^{3,6} for 2-pentanone, 3-pentanone, and 2-hexanone. These discrepancies are not dependent on the reference reaction used in the relative rate measurements, and they could be ascribed to systematic errors in at least one of these kinetic studies.⁶

For methyl butanone there is only one reported experimental value of k .¹¹

In this work we have performed a mechanistic and kinetic study of the reactions of three ketones with OH radicals—propanone, 2-pentanone, and methyl butanone—in the temperature range 280–440 K:



For each ketone a complex system with several pathways, which move through different transition structures to a set of various products, is presented. To simplify its analysis, we have assumed that once a specific pathway started it proceeds to completion, independently of the other pathways; i.e., there is no mixing or crossover between different pathways. On this basis, the overall rate constant (k) that measures the rate of OH disappearance can be determined by summing up the rate coefficients calculated for each different pathway.²⁵ In addition, in this paper the temperature dependence of k has been studied, and the Arrhenius parameters have been calculated.

The aim of our work was to study the site reactivity of the studied ketones toward the hydroxyl radical. We intend not only to explain the site reactivity and to find the hydrogen atoms most likely to be abstracted but also to discern the reasons for such preference.

Computational Methods

Each reaction channel was modeled taking into account the conformation of the abstracted H atom. Taking the carbonyl group as reference, two possible orientations have been considered in the transition states. As it was previously proposed for OH + propanone reaction study:²⁶

Eclipsed: The hydrogen atom is in the eclipsed conformation with respect to the carbonyl group. This orientation leads to a possible attractive interaction between the H atom in the OH radical and the O atom in the >C=O group.

Alternated: The dihedral angle between the hydrogen to be abstracted and the oxygen atom in the carbonyl group is about 120° or -120° . This orientation prevents possible interactions between the OH radical and the >C=O group.

Electronic structure calculations have been performed with the Gaussian 98²⁷ programs package. Full geometry optimizations were made for all the stationary points using the BHandHLYP hybrid HF-density functional²⁸ and the 6-311G(d,p) basis set. This functional was chosen on the base of its proven effectiveness,^{29–42} and the energies were improved by single point calculations at the CCSD(T)/6-311G(d,p) level. Restricted calculations were used for closed-shell systems and unrestricted ones for open-shell systems.

Frequency calculations were carried out for all the stationary points at the corresponding level of theory. Local minima and

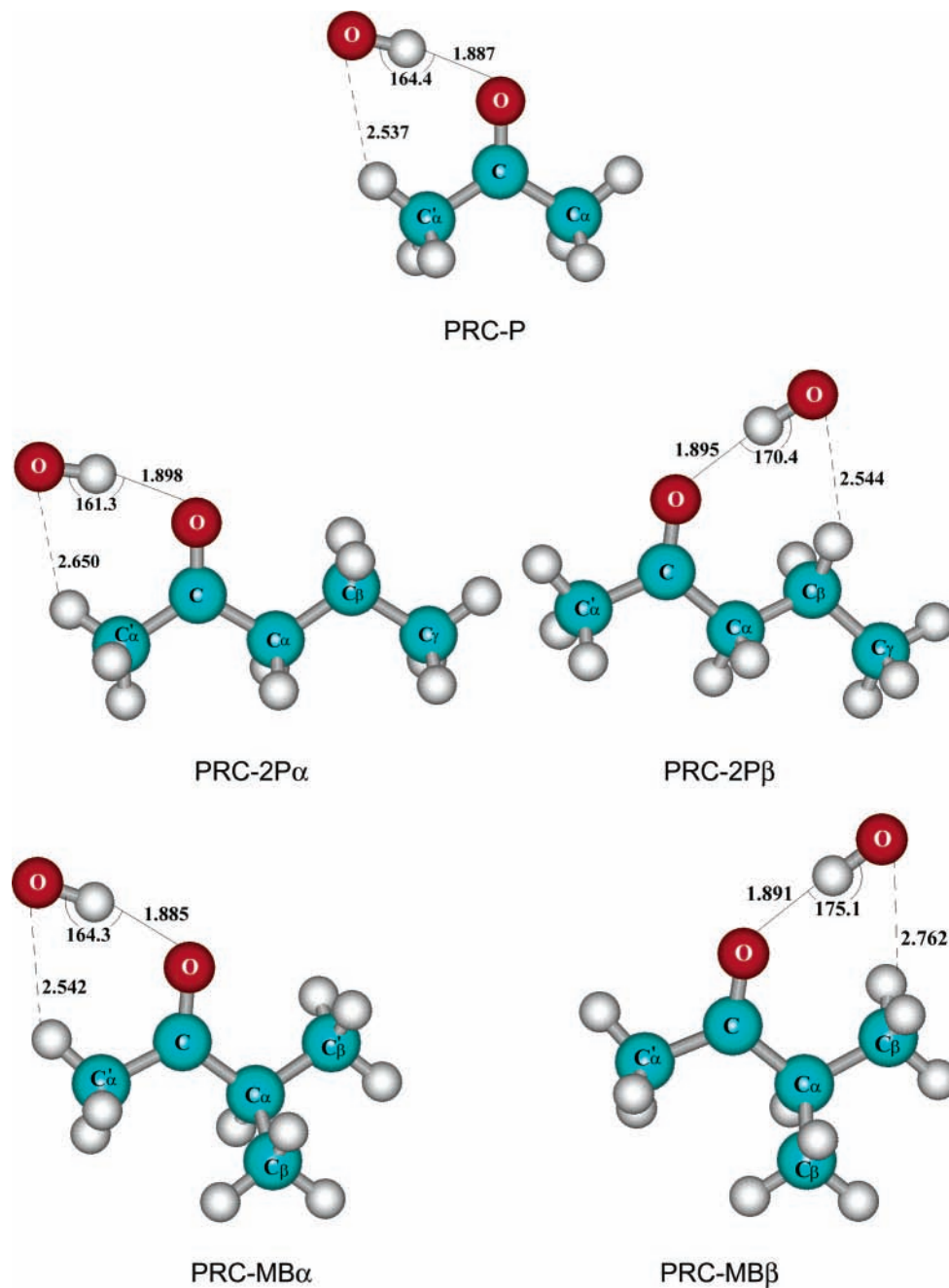


Figure 2. Fully optimized geometry of prereactive complexes.

transition states were identified by the number of imaginary frequencies (NIMAG = 0 or 1, respectively). In addition, the vibrational modes of transition states were inspected using the GaussView program, and it was confirmed that they do connect the corresponding reactants and products. Zero-point energies (ZPE) and thermal corrections to the energy (TCE) were included in the determination of energy barriers.

The conventional transition state theory (TST),^{43,44} implemented in the Rate 1.1 program,⁴⁵ was used to calculate the rate coefficients since it has the advantage of being inexpensive for a high level of ab initio calculations.

The tunneling correction defined as the Boltzmann average of the ratio of the quantum and the classical probabilities was calculated using the Eckart method.⁴⁶ This method approximates the potential by a one-dimensional function that is fitted to reproduce the zero-point energy corrected barrier, the enthalpy of reaction at 0 K, and the curvature of the potential curve at

the transition state. This method tends to overestimate the tunneling contribution, especially at very low temperature, because the fitted Eckart function is often too narrow. However, sometimes it compensates for the corner-cutting effect not included in the Eckart approach.^{47–49} Such compensation can lead to Eckart transmission coefficients similar⁴⁸ or even lower⁴⁹ than those obtained by the small-curvature tunneling (SCT) method⁵⁰ at temperatures equal to or higher than 300 K.

Results and Discussion

Geometries. Because of the large number of structures modeled and the structural similarity among the equivalent stationary points studied in this work, we are not going to analyze them separately.

All the prereactive complexes (PRC) studied here are shown in Figure 2. The PRCs correspond to abstractions of eclipsed

TABLE 1: L Parameter for Ketones + OH Reactions

	H orientation	propanone	2-pentanone	methyl butanone
C_α (primary)	eclipsed	0.72	0.69	0.66
	alternated	0.47	0.45	0.43
C_α (secondary)	alternated		0.33	
C_α (tertiary)	alternated			0.26
C_β (primary)	eclipsed			0.62
	alternated			0.51
C_β (secondary)	eclipsed		0.48	
C_γ (primary)	alternated		0.48	

H atoms. The PRCs connecting reactants and alternated transition states are so similar in energy to the isolated reactants that they can be neglected in the modeling. Consequently, the alternated abstractions have been modeled as direct abstractions: isolated reactants (R) \rightarrow TS \rightarrow products (P).

The fully optimized geometries of eclipsed PRCs show ringlike structures, as previously proposed.^{4,13} The complex formation is caused by two attractive interactions. The main one occurs between the H atom in the OH radical and the O atom in the carbonyl group. For all the modeled systems these atoms are 1.89 Å apart, which represents a hydrogen bond interaction, and it is responsible for the stabilization. The other interaction is found between the O in OH and one of the hydrogens in the ketone. The O \cdots H distance is about 2.5 Å, which is too large for a hydrogen bond interaction. This distance is longer than the previous one because hydrogens bonded to C atoms are not positive enough to strongly interact with an O atom. Consequently, the interaction is much weaker.

Prereactive complexes may involve either beta hydrogens or terminal C_α hydrogens. The difference between alpha and beta complexes lies in the number of members forming the ring. For nonsymmetric ketones, such as methyl butanone, two PRCs are found: one with the O in OH pointing to an H in the methyl group linked to C_α (PRC-MB α , in Figure 2) and the other with the O in OH pointing to an H in the C_β of the ethyl group (PRC-MB β , in Figure 2). For 2-pentanone two PRCs are also found (PRC-2p α and PRC-2p β , in Figure 2). According to the PRCs geometrical features, the only abstractions that can connect with the transition states are those involving either H atoms linked to a C_β or hydrogens linked to a C_α in an eclipsed orientation.

The eclipsed transition states present a hydrogen-bond-like interaction between the H atom in the OH radical and the O atom in the carbonyl group. This interaction should stabilize the eclipsed TS and play a relevant role in the abstractions of the hydrogens oriented that way.

Two general features of the transition states are relevant to our discussion: (1) the position of the TS on the reaction coordinate and (2) for eclipsed transition states the distance between the H in OH and the O in the carbonyl group, which is a measure of the strength of the corresponding interaction.

The L parameter,^{51,52} defined as

$$L = \frac{\delta r(\text{CH})}{\delta r(\text{HO})} \quad (1)$$

indicates whether a transition-state structure is early ($L < 1$) or late ($L > 1$), and it also quantifies the corresponding trend. In eq 1 $\delta r(\text{CH})$ represents the variation in the breaking bond distance when going from transition state to reactants, while $\delta r(\text{HO})$ represents the variation in the forming bond distance when going from transition state to products. Thus, the L parameter is useful to quantify feature 1, above. In this work, L parameters have been calculated for all the modeled channels (Table 1). The TSs corresponding to abstractions from primary

carbons (Figure 3a) are the latest for each ketone, regardless of their position with respect to the carbonyl group. Thus, one would expect that all primary abstractions have similar energy barriers. The TSs corresponding to abstractions from secondary carbons (TS-2P α 2 and TS-2P β 2 in Figure 3b) are intermediate, while the ones corresponding to abstraction from the tertiary carbon in methyl butanone (TS-MB α 3 in Figure 3b) has the smallest L value, equal to 0.26. According to these results, the earliness of the TS cannot explain, by itself, the larger reactivity of the beta site in 2-pentanone. The earlier the TS, the lower the energy barrier of the corresponding path, provided that there are no other factors affecting otherwise. The reactivity order should then be tertiary $>$ secondary $>$ primary, with similar reactivities for any hydrogen bonded to C equivalently substituted, which is exactly the behavior that is observed in the alkanes + OH reactions.

The TSs can also be divided into three groups with respect to the comparative parameter corresponding to the distance between the H in the OH and the O in the carbonyl group (feature 2, above). This H \cdots O distance determines the strength of the interaction, and consequently, it influences the height of the barrier. In increasing order, the first group includes the TSs corresponding to abstractions from beta carbons ($d_{\text{H}\cdots\text{O}} \approx 2.10$ Å), the second group involves the TSs related to primary alpha abstractions ($d_{\text{H}\cdots\text{O}} \approx 2.25$ Å), and the third group includes secondary and tertiary alpha TSs ($d_{\text{H}\cdots\text{O}} \approx 3.6$ Å). According to this, it seems that this feature could be responsible for the peculiar positional reactivity of ketones in their reactions with OH radical.

Considering both TS features together, as quantified by parameters L and $d_{\text{H}\cdots\text{O}}$, one can say that H atoms bonded to primary C_β are more likely to be abstracted by an OH radical than those linked to primary C_α . The reason for that behavior is that both abstractions involve TSs with similar positions on the reaction coordinate, but the H \cdots O distance is shorter when the abstraction occurs at a beta site. Analogously, an H abstraction is more likely to occur from a secondary C_β than from a secondary C_α . It is not always possible to make this kind of prediction, based on the two geometrical features discussed above, because features 1 and 2 may act in opposite directions. For instance, the comparison between a secondary C_β and a tertiary C_α is ambiguous because feature 1 favors the latter, while feature 2 favors the former. In this case the size of the energy barriers and the rate coefficients will be used.

Energies. The geometric features discussed above influence the values of the relative energies reported in Table 2. The reaction profiles corresponding to those energies are shown in Figure 4.

As mentioned before, the mechanism of each abstraction was modeled by a different mechanism, according to whether the H to be abstracted is eclipsed or alternated with respect to the carbonyl group. The eclipsed mechanism was modeled as R \rightarrow PRC \rightarrow TS \rightarrow P, while the alternated mechanism was modeled as R \rightarrow TS \rightarrow P. Consequently, some abstractions have been modeled exclusively as direct abstractions, others as two-step abstractions, and others as a combination of both (mixed abstraction), depending on the structure of the studied ketone.

For many reactions the energy barriers correlate with the reaction enthalpies (ΔH). Such correspondence has been used to estimate rate constants, see e.g. ref 53, based on the Evans and Polanyi work.⁵⁴ However, for most of the VOCs + OH hydrogen abstraction reactions, and in particular for the ketones + OH reactions, this relation is not fulfilled. For the latter, the forming bond is always the same (O–H), and differences in

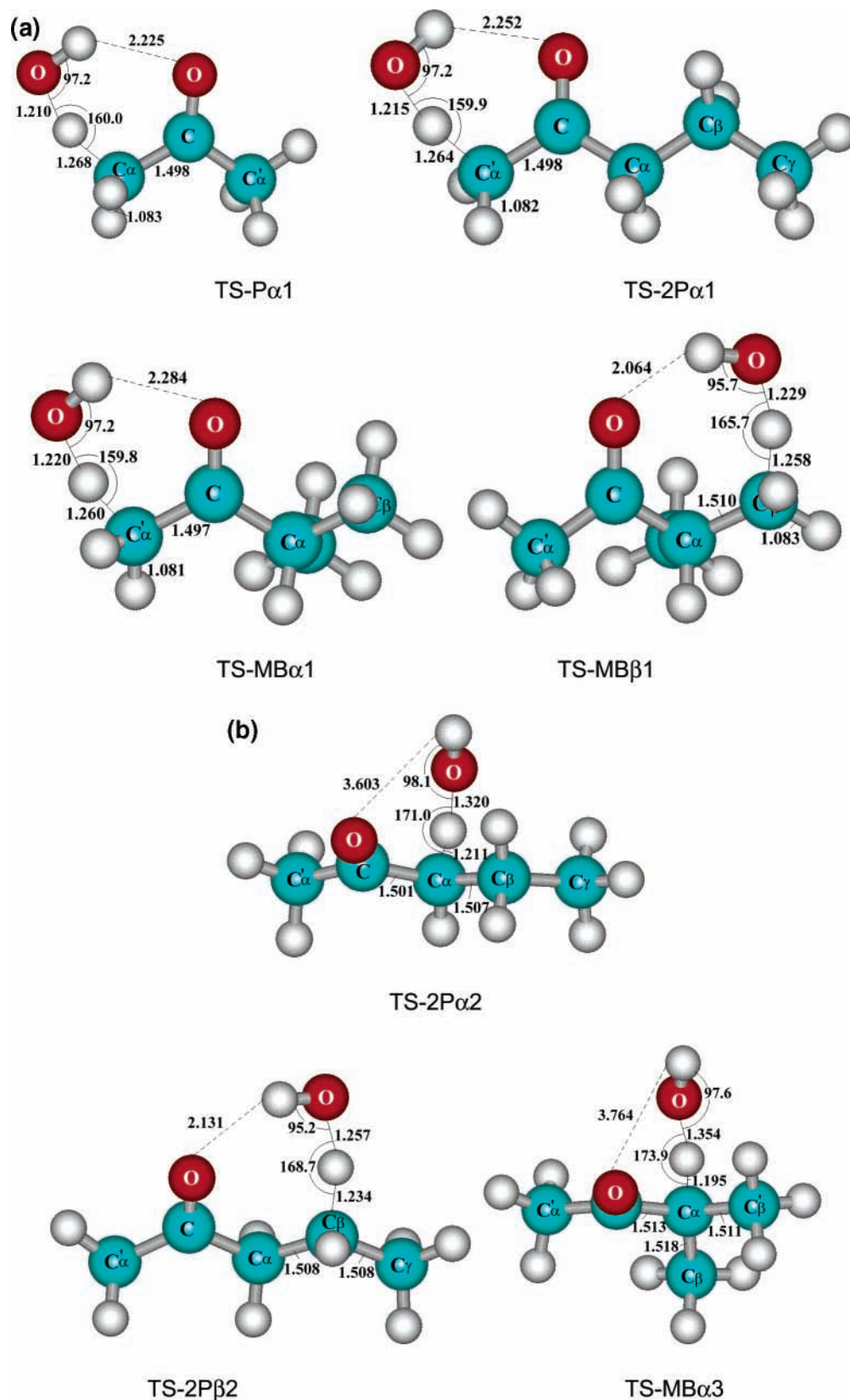


Figure 3. (a) Fully optimized geometry of most important transition states corresponding to abstractions from primary carbons. (b) Fully optimized geometry of most important transition states corresponding to abstractions from nonprimary carbons.

reaction enthalpies among the diverse abstraction sites depend only on the breaking bond strength, which is in turn influenced by the degree of substitution at the carbon atoms and by the proximity to the carbonyl group. Therefore, the most stable product radical is expected to occur for H abstraction from the

most substituted alpha carbons. Accordingly, the abstraction from the tertiary C α in methyl butanone should be the most exothermic reaction, for the set of ketones studied in this work.

The reaction barriers do not show the same behavior (Figure 4a,b), not even in a qualitative way. The reason is that they

TABLE 2: Relative Energies with Respect to the Isolated Reactants for Each Abstraction Channel Reported in kcal/mol and Calculated at CCSD(T)//BHandHLYP/6-311G(d,p); ZPE Corrections Are Included

ketone	reaction site	H		E_{Stab}^a	E_{Barr}^a	E_{HR}^a
		orientation				
propanone	alpha primary	eclipsed		-6.06	3.77	-16.78
		alternated			4.00	
2-pentanone	alpha primary	eclipsed		-6.08	3.50	-16.73
		alternated			3.73	
	alpha secondary	alternated			1.07	-20.83
	beta secondary	eclipsed		-6.08	-0.39	-14.56
methyl butanone	gamma primary	alternated			4.44	-12.37
	alpha primary	eclipsed		-6.00	3.33	-17.11
		alternated			3.56	
	alpha tertiary	alternated			0.10	-23.86
	beta primary	eclipsed		-6.00	0.76	-11.56
alternated				3.45		

$$^a E_{\text{Stab}} = E_{\text{PRC}} - E_{\text{Reac}}, E_{\text{Barr}} = E_{\text{TS}} - E_{\text{Reac}}, E_{\text{HR}} = E_{\text{Prod}} - E_{\text{Reac}}.$$

depend not only on the bonds strength but also on dynamic factors, which influence the transition states energy but not the products energy. One dynamic factor, already discussed in the previous section, is the hydrogen-bond-like interaction found in the transition states. The occurrence and strength of such interactions depend on the relative position between the H to be abstracted and the O in the carbonyl group. As mentioned before, the strongest interaction is found in beta transition states. Thus, the energy barriers corresponding to beta abstractions are always lower than those corresponding to alpha abstractions (Table 2), provided that the degree of substitution is the same.

The comparison among the calculated reaction barriers can be very useful to determine the relevance of the different factors influencing the site reactivity in ketones and to find an explanation to the special features of their reactivity.

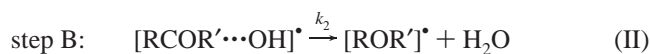
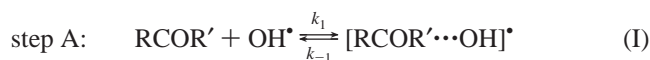
Analyzing in detail the energetic values (Table 2), it can be seen that, among all the abstraction channels studied in this work, the lowest net energy barrier (-0.4 kcal/mol) corresponds to the abstraction from the secondary C_β in 2-pentanone, while its thermal effect is only of -15.55 kcal/mol. On the other hand, the tertiary C_α in methyl butanone has the weakest bond and consequently the largest thermal effect (-23.86 kcal/mol), while its energy barrier is 0.10 kcal/mol. Taking into account all the values reported in Table 2 together, it is clear that for ketones + OH reactions there is no correspondence between the energy barriers and the reaction enthalpies. Consequently, in this case the rate constants and the activation energies should not be estimated on the basis of the Evans and Polanyi work.⁵⁴

Unlike the geometrical features, the energy barriers (E_{Barr}) allow the comparison between sites that differ in their degree of substitution and in their position with respect to the >C=O group. Because of the nature of the two factors influencing the site reactivity, it is interesting to compare the tertiary alpha site in methyl butanone with the secondary beta site in 2-pentanone. According to our results $E_{\text{Barr}}^{\text{TertC}\alpha}(\text{methyl butanone}) > E_{\text{Barr}}^{\text{SecC}\beta}(\text{2-pentanone})$ by 0.35 kcal/mol, suggesting that the position of the reacting site with respect to the >C=O group has a larger influence on reactivity than the degree of substitution of the carbon atom. Comparing secondary alpha sites and primary beta sites, it can be seen that barrier values follow the order $E_{\text{Barr}}^{\text{SecC}\alpha}(\text{2-pentanone}) > E_{\text{Barr}}^{\text{PrimC}\beta}(\text{methyl pentanone})$.

The differences in energy barriers among all the modeled channels for each ketone are quite small, implying that more than one channel is involved in the reaction. It is important to emphasize this because, despite their chemical similarity, the

aldehydes + OH reactions occur only by abstraction of the aldehydic H.^{20,55} However, the ketones multiple-path mechanism has a preferred channel, which is not unique for all of them and which depends on the chemical structure of the specific ketone reacting with the OH radical. Nevertheless, some generalizations can be made. Comparing only alpha and beta sites, and extrapolating our results, the site reactivity should decrease in the following order: tertiary C_β s (not modeled) > secondary C_β s \approx tertiary C_α s > primary C_β s \approx secondary C_α s > primary C_α s > primary C_γ s. The reactivity of sites further than gamma should be lower than those analyzed here (provided that the degree of substitution is the same) and similar to the reactivity of equivalent sites in alkanes.

As shown in Figure 4a, the mechanism of the ketones + OH eclipsed abstractions seems to be a two-step mechanism. The relatively high stabilization energies of the prereactant complex (PRC) (about 6 kcal/mol, Table 2) show unambiguously that the mechanism is complex, with a first reversible step leading to the PRC formation and a second irreversible step yielding the corresponding radical and water. The proposed mechanism is



The energy barriers of the second step are all positive and higher than 5.7 kcal/mol for all the studied cases (Table 2), suggesting that the tunneling effect can be relevant in the ketones + OH reactions.

Kinetics. The rate constant (k) corresponding to all the studied reaction channels can be analyzed in terms of TST. As in previous works for similar mechanisms,^{18,20-22} we have assumed that in the eclipsed channels the prereactant complex undergoes collisional stabilization; i.e., this reaction step occurs in a high-pressure limit. Recently Masgrau et al.²⁶ have used the low-pressure limit case to calculate the rate constant of propanone. Though they used the state of the art on quantum chemical calculations and VTST, they did not reproduce the temperature dependence, specially at low T . At the time this article was in review process, another article on propanone + OH reaction, including experimental and theoretical results, has been published.⁵⁶ The authors properly reproduced the experimental temperature dependence of the rate coefficient by using the high-pressure approach, VTST, and almost the same level of calculation that was used in ref 26. Figure 5 shows Arrhenius plots from the experimental data,⁵⁷ compared to both theoretical approaches, low²⁶ and high⁵⁶ pressure. The numerical data corresponding to ref 56, which is not in the original article, was kindly provided by Professor Paul Marshall. Nevertheless, Marshall et al.⁵⁶ concluded that the reaction does not occur in the high-pressure regime on the basis of their independent RRRK results. Therefore, our high-pressure assumption is made though the validity of this assumption is in some doubt.

According to the reaction mechanism proposed above for eclipsed H abstractions, if k_1 and k_{-1} are the forward and reverse rate constants for the first step and k_2 corresponds to the second step, a steady-state analysis leads to a rate coefficient for each overall reaction channel which can be written as

$$k = \frac{k_1 k_2}{k_{-1} + k_2} \quad (\text{2})$$

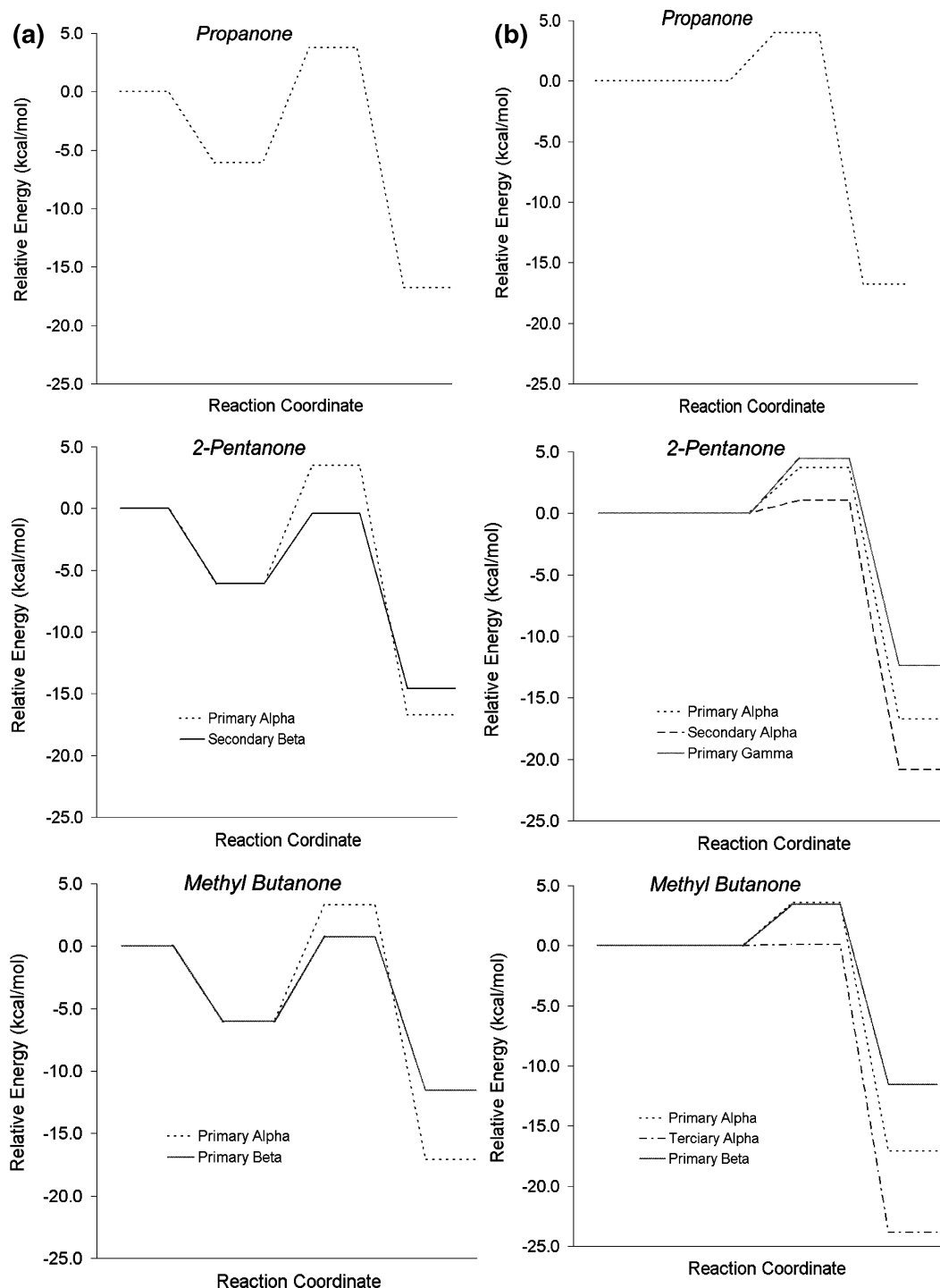


Figure 4. (a) Energetic profiles for the OH eclipsed hydrogen abstractions from ketones. (b) Energetic profiles for the OH alternated hydrogen abstractions from ketones.

Even though the energy barrier for k_{-1} is about the same size as that for k_2 , the entropy change is much larger in the reverse reaction than in the formation of the products. Thus, it should be expected a k_{-1} considerably larger than k_2 . On the basis of this assumption, first considered by Singleton and Cvetanovic,⁵⁸ k can be rewritten as

$$k = \frac{k_1 k_2}{k_{-1}} = \frac{A_1 A_2}{A_{-1}} \exp[-(E_1^* + E_2^* - E_{-1}^*)/RT] \quad (3)$$

where E_1^* and E_{-1}^* are the step 1 energy barriers, corresponding to the forward and reverse directions, respectively.

Since E_1^* is zero, the net (or apparent) energy barrier for the overall reaction channel is

$$E^* = E_2^* - E_{-1}^* = (E_{\text{TS}} - E_{\text{RC}}) - (E_{\text{R}} - E_{\text{RC}}) = E_{\text{TS}} - E_{\text{R}} \quad (4)$$

where E_{TS} , E_{RC} , and E_{R} are the total energies of the transition state, the reactant complex, and the reactants, respectively.

Applying basic statistical thermodynamic principles, the equilibrium constant (k_1/k_{-1}) of the fast preequilibrium between

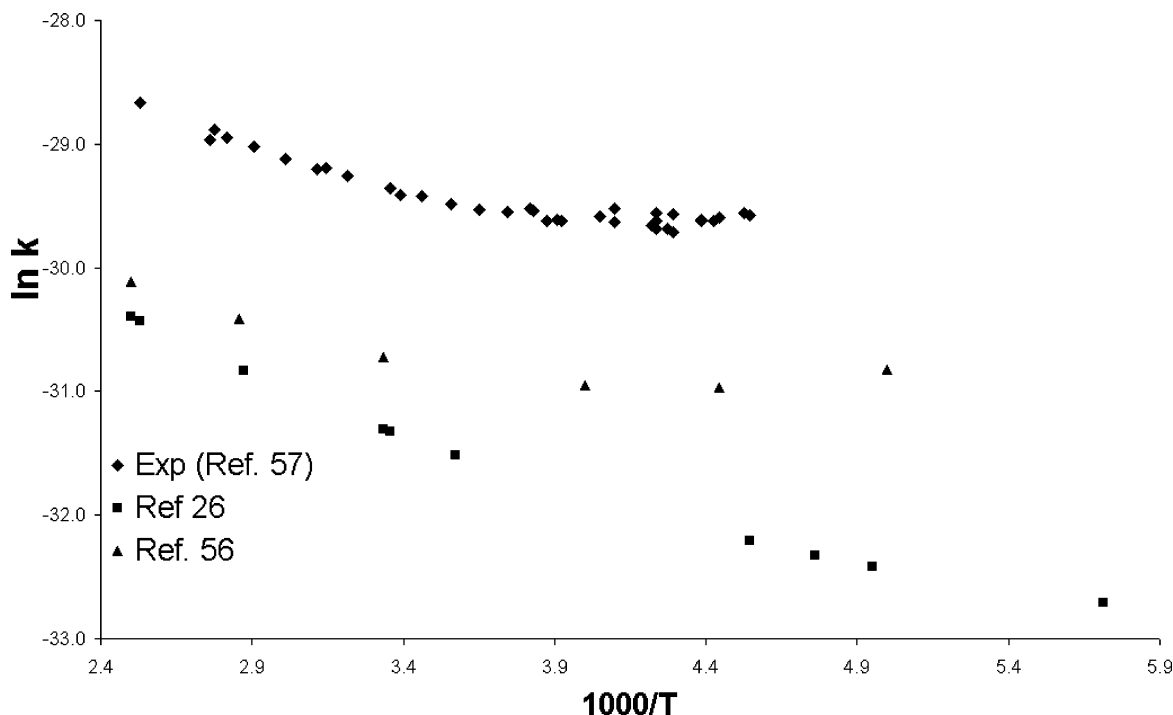


Figure 5. Comparison between experimental and theoretical rate coefficients using both high- and low-pressure approaches from refs 26 and 56.

the reactants and the reactant complex may be obtained as

$$K_{\text{eq}} = \frac{Q_{\text{RC}}}{Q_{\text{R}}} \exp[(E_{\text{R}} - E_{\text{RC}})/RT] \quad (5)$$

where Q_{RC} and Q_{R} represent the partition functions corresponding to the reactant complex and the isolated reactants, respectively.

In a unimolecular process, under high-pressure conditions, an equilibrium distribution of reactants is established, and the CTST formula can be applied⁵⁹ to calculate k_2 :

$$k_2 = \kappa_2 \frac{k_{\text{B}} T}{h} \frac{Q_{\text{TS}}}{Q_{\text{RC}}} \exp[(E_{\text{RC}} - E_{\text{TS}})/RT] \quad (6)$$

where κ_2 is the tunneling factor, k_{B} and h are the Boltzmann and Planck constants, respectively, and Q_{TS} is the transition-state partition function. The energy difference include the ZPE corrections. The effective rate coefficient of each channel is then obtained as

$$k = \sigma K_{\text{eq}} k_2 \quad (7)$$

where σ is the symmetry factor, which is related to the reaction path degeneracy and its value depends on the H atom to be abstracted. The symmetry factor is obtained by imaging all identical atoms to be labeled and by counting the number of different but equivalent arrangements that can be made by rotating (but not reflecting) the molecule.⁶⁰

Finally, the overall rate constant (k) for each ketone can be determined by summing up the rate coefficients calculated for the different modeled pathways.²⁵ The rate coefficient for each mixed abstraction channel has been obtained by adding up the corresponding eclipsed and alternated rate coefficients. They have been calculated separately, and the proper symmetry factor was used in each case. The k values were calculated over the temperatures range 280–440 K.

Some authors have proposed that, since the stabilization of the reactant complexes is less important than the entropy change,

they are too short-lived species to be taken into account in the mechanism.⁶¹ This could be true at high temperatures; nevertheless, they have been considered here in the K_{eq} calculations. Indeed, short-lived intermediates are of crucial importance in most organic reaction mechanisms. The idea that short-lived species should not be taken into account because of their short lifetime is in contradiction even with the transition-state theory, which assumes an “equilibrium” involving the species with the shortest lifetime, i.e., the transition state. Some OH weakly bound complexes have been experimentally identified.^{14,15}

In addition, the complex mechanism described above seems to be common to many OH reactions with unsaturated, oxygenated, and nitrogenated organic compounds.^{18–22,39–41,62,63} Its importance has been reviewed recently.^{16,17}

Since the rate coefficient analysis includes the influence of entropic factors on the reactivity, it provides a more complete approach to chemical reactions than mere energetic considerations. The entropy changes, as well as the tunneling effect, could lead to a site reactivity order different than the one expected by taking into account only energy barriers.

The rate coefficients calculated at 298 K and the Arrhenius parameters calculated over the temperature range 280–440 K are reported in Table 3, as well as the corresponding experimental values, to calibrate the quality of our results. The rate coefficient temperature dependence was fitted in this work by a two-parameters equation [$k = A \exp(-B/T)$]. The agreement between experimental and calculated overall rate coefficients is good, as is shown in Table 3. This agreement supports the mechanism proposed above. On the other hand, the good agreement with experimental values is also a confirmation of the accuracy of the chosen method (CCSD(T)//BHandHLYP/6-311G(d,p)) within the TST approximation and for rate coefficient calculations of OH hydrogen abstraction reactions. A good agreement between the theoretical and recommended Arrhenius parameters is also found, although the calculated activation energies and the preexponential factors are in general slightly overestimated. In addition, the available experimental and calculated reactivity orders coincide.

TABLE 3: Overall CTST Arrhenius Parameters for Ketones + OH Radical Gas Phase Reactions, Determined over the Temperature Range 280–440 K; Branching Ratios ($\Gamma = k_{\text{partial}}/k_{\text{overall}} \times 100$) at 298 K

	propanone	2-pentanone	methyl butanone
k_{exp} (cm ³ molecule ⁻¹ s ⁻¹)	(1.9 ± 0.3) × 10 ^{-13 a} 2.21 × 10 ^{-13 b} 1.90 × 10 ^{-13 c} 2.27 × 10 ^{-13 d}	(4.00 ± 0.28) × 10 ^{-12 d} (4.98 ± 0.25) × 10 ^{-12 e}	3.02 × 10 ^{-12 c}
k_{calc} (cm ³ molecule ⁻¹ s ⁻¹)	1.92 × 10 ⁻¹³	2.38 × 10 ⁻¹²	2.30 × 10 ⁻¹²
$E_{\text{exp}}^{\text{Arr}}$ (kcal/mol)	1.03 ± 0.40 ^a 1.361 ± 0.204 ^b 1.115 ± 0.111 ^c 1.192 ± 0.143 ^d	NA	-0.384 ± 0.13 ^c
$E_{\text{calc}}^{\text{Arr}}$ (kcal/mol)	1.96	-0.48	0.80
A_{exp} (cm ³ molecule ⁻¹ s ⁻¹)	1.1 × 10 ^{-12 a} 2.20 × 10 ^{-12 b} (1.25 ± 0.23) × 10 ^{-12 c} (1.70 ± 0.41) × 10 ^{-12 d}	NA	(1.58 ± 0.35) × 10 ^{-12 c}
A_{calc} (cm ³ molecule ⁻¹ s ⁻¹)	5.18 × 10 ⁻¹²	1.02 × 10 ⁻¹²	8.75 × 10 ⁻¹²
Γ		$\alpha_{\text{primary}} = 4.9\%$ $\alpha_{\text{secondary}} = 7.0\%$ $\beta_{\text{secondary}} = 82.1\%$ $\gamma_{\text{primary}} = 6.0\%$	$\alpha_{\text{primary}} = 17.2\%$ $\alpha_{\text{tertiary}} = 27.9\%$ $\beta_{\text{primary}} = 54.9\%$

^a Reference 9. ^b Reference 10. ^c Reference 11. ^d Reference 4. ^e Reference 6

The partial rate coefficients cannot be determined experimentally because reactions occur simultaneously, and in some cases they even lead to the same products. Thus, the experimental data are mostly available only for the overall reactions. That is why theoretical methods can be so valuable for the full understanding of the chemical systems, provided that they have previously proved their reliability. The comparison between experimental and calculated overall data is in most cases the only available criterion for that purpose. Therefore, the good agreement between experimental and calculated (overall) results obtained in this work supports the quality of the kinetic data obtained. This good agreement also justifies the use of the partial rate constants (corresponding to each independent channel) in the study of the reasons which can cause the peculiar reactivity in ketones + OH reactions. Since the number of H in each abstraction site differs in most of the organic molecules, it is also useful to calculate the k values normalized to one H atom. This will facilitate the analysis and comparison of the site reactivities.

The calculated branching ratios, defined for each channel as

$$\Gamma = \frac{k_{\text{partial}}}{k_{\text{overall}}} \times 100 \quad (8)$$

are also shown in Table 3. For 2-pentanone the abstraction from the beta site is found to be dominant. This result agrees with the experimental evidence.^{3–7,11} Since there is another secondary carbon in this molecule, this finding supports the idea that the position relative to the >C=O group has more influence on the site reactivity than the degree of substitution. However, the influence of the latter is shown in our results by the finding that the abstraction from a secondary C_α is about 2.5% more favored than the abstraction from a primary C_α. For methyl butanone the primary beta channel is found to be the most likely to occur. According to our results, 54.9% of the abstractions occur at this site compared to 27.9% at the tertiary alpha carbon. In this case the percentages do not reflect correctly the reactivity of the corresponding sites because there are six hydrogen atoms linked to primary C_β and only one H linked to tertiary C_α. Normalizing to one eclipsed H atom, the Γ value for each H becomes $\Gamma(\text{C}_{\alpha,\text{tertiary}}) = 27.9\%$ and $\Gamma(\text{C}_{\beta,\text{primary}}) = 18.3\%$.

The kinetic data, normalized to one H atom, are listed in Table 4 for the mixed channels. With the purpose of quantifying the influence of the stabilizing interaction present in the TS

TABLE 4: Comparison between Eclipsed and Alternated Rate Coefficients at 298 K, Corresponding to Mixed Abstractions, Normalized to One H Atom

site	ketone	rate coeff (cm ³ molecule ⁻¹ s ⁻¹)	
		eclipsed	alternated
primary alpha	propanone	7.51 × 10 ⁻¹⁴	1.05 × 10 ⁻¹⁴
	2-pentanone	9.06 × 10 ⁻¹⁴	1.26 × 10 ⁻¹⁴
	methyl butanone	3.09 × 10 ⁻¹³	4.32 × 10 ⁻¹⁴
primary beta	methyl butanone	4.02 × 10 ⁻¹³	1.97 × 10 ⁻¹⁴

structures, we have calculated the ratio between the normalized rate coefficients corresponding to eclipsed and alternated abstractions:

$$\mathcal{R} = \frac{k_{\text{eclipsed}}}{k_{\text{alternated}}} \quad (9)$$

It is helpful to remember that this attractive interaction takes place between the H in the OH radical and the O in the -C=O group, and therefore, it can occur in the eclipsed orientation but not in the alternated one.

The ratio values are found to be about 7 for alpha sites and about 20 for beta sites. The fact that $\mathcal{R} > 1$ can be explained by the stabilization in the eclipsed TS and by the complex mechanism (R → PRC → TS → P), which leads to tunneling corrections considerably larger than in the direct mechanism (R → TS → P).

The much larger value of $\mathcal{R}^{\text{beta}}$ compared to $\mathcal{R}^{\text{alpha}}$ is consistent with the finding that the stabilizing interaction present in beta transition states is much stronger than the equivalent interaction in alpha transition states. It is also in line with the result that the net barrier for the eclipsed beta channel is 2.7 kcal lower than that for the alternated channel.

Conclusions

The good agreement between calculated and available experimental data shows that CCSD(T)//BHandHLYP/6-311G-(d,p) calculations, within TST methodology, properly describe the systems studied in this work.

The presence of a prereactive complex in the abstraction channels involving beta hydrogens and eclipsed alpha hydrogens is confirmed. The prereactive complexes show ringlike structures, and they are caused by two attractive interactions. The strongest one occurs between the H atom in the OH radical and the O atom in the carbonyl group. The weakest one is

formed between the O in OH and one of the hydrogens in the ketone. For nonsymmetric ketones two PRCs are found.

Two different mechanisms have been modeled (complex: $R \rightarrow PRC \rightarrow TS \rightarrow P$; direct: $R \rightarrow TS \rightarrow P$) depending on the orientation of the H to be abstracted (either eclipsed or alternated with respect to the C=O group). The presence of a PRC in the complex mechanism increases the energy barrier of the second step and leads to a larger tunneling effect, while the apparent barrier remains the same. Consequently, the presence of a PRC increases the corresponding rate coefficient.

The eclipsed and alternated net (as measured from reactants) energy barriers corresponding to the same site of abstraction, differ by about 0.2 and 2.4 kcal/mol for alpha and beta sites, respectively. The larger difference for beta sites is caused by the stronger interaction in the TS, showing that the presence of such interaction in the transition structures is responsible for the "anomalous" increase of the beta sites reactivity. In consequence, the ratios between the corresponding normalized rate coefficients are found to be 7 and 20 for alpha and beta abstractions, respectively.

Finally, although prereactive complexes enhance the tunneling factor and lead to increased rate coefficients, in the case of ketones the most important factor explaining the observed reactivity is to be found in the hydrogen bonds in the structure of the TSs for beta abstractions.

Acknowledgment. The authors gratefully acknowledge the financial support from the Instituto Mexicano del Petróleo (IMP) through project D00179. We also thank the IMP Computing Center for supercomputer time on SGI Origin 3000 and on SGI Origin 2000. We thank professors W. T. Duncan, R. L. Bell, and T. N. Truong for providing The Rate program through the Internet.

References and Notes

- http://www.epa.gov/triexplorer/chemical.htm (data update as of Aug 1, 2001).
- http://homepages.luc.edu/~mschmel/Handout8.pdf.
- Atkinson, R.; Aschmann, S. M.; Carter, W. P. L.; Pitts, J. N., Jr. *Int. J. Chem. Kinet.* **1982**, *14*, 839.
- Wallington, T. J.; Kurylo, M. J. *J. Phys. Chem.* **1987**, *91*, 5050.
- Dagaut, P.; Wallington, T. J.; Liu, R.; Kurylo, M. J. *J. Phys. Chem.* **1988**, *92*, 4375.
- Atkinson, R.; Aschmann, S. M. *J. Phys. Chem.* **1988**, *92*, 4008.
- Atkinson, R.; Aschmann, S. M. *Int. J. Chem. Kinet.* **1995**, *27*, 261.
- Kwok, E. S. C.; Atkinson, R. *Atmos. Environ.* **1995**, *29*, 1685.
- Atkinson, R. D.; Baulch, L.; Cox, R. A.; Hampson, R. F., Jr.; Kerr, J. A.; Rossi, M. J.; Troe, J. *J. Phys. Chem. Ref. Data* **1999**, *28*, 191.
- DeMore, W. B.; Sander, S. P.; Golden, D. M.; Hampson, R. F.; Kurylo, M. J.; Howard, C. J.; Ravishankara, A. R.; Kolb, C. E.; Molina, M. J. Chemical kinetics and photochemical data for use in stratospheric modeling 1997. Evaluation number 12 JPL Publication 97-4.
- Le Calvé, S.; Hitier, D.; Le Bras, G.; Mellouki, A. *J. Phys. Chem. A* **1998**, *102*, 4579.
- Atkinson, R. *Int. J. Chem. Kinet.* **1987**, *19*, 799.
- Klamt, A. *Chemosphere* **1996**, *32*, 717.
- Loomis, R. A.; Lester, M. I. *J. Chem. Phys.* **1995**, *103*, 4371.
- Lester, M. I.; Pond, B. V.; Anderson, D. T.; Harding, L. B.; Wagner, A. F. *J. Chem. Phys.* **2000**, *113*, 9889.
- Smith, I. W. M.; Ravishankara, A. R. *J. Phys. Chem. A* **2002**, *106*, 4798.
- Hansen, J. C.; Francisco, J. S. *Chem. Phys. Chem.* **2002**, *3*, 833.
- Alvarez-Idaboy, J. R.; Mora-Diez, N.; Vivier-Bunge, A. *J. Am. Chem. Soc.* **2000**, *122*, 3715.
- Uc, V. H.; García-Cruz, I.; Hernández-Laguna, A.; Vivier-Bunge, A. *J. Phys. Chem. A* **2000**, *104*, 7847.
- Alvarez-Idaboy, J. R.; Mora-Diez, N.; Boyd, R. J.; Vivier-Bunge, A. *J. Am. Chem. Soc.* **2001**, *123*, 2018.
- Galano, A.; Alvarez-Idaboy, J. R.; Montero-Cabrera, L. A.; Vivier-Bunge, A. *J. Comput. Chem.* **2001**, *22*, 1138.
- Galano, A.; Alvarez-Idaboy, J. R.; Bravo-Pérez, G.; Ruiz-Santoyo, M. E. *THEOCHEM* **2002**, *617*, 77.
- Frank, I.; Parinello, M.; Klamt, A. *J. Phys. Chem. A* **1998**, *102*, 3614.
- Cox, R. A.; Patrick, K. F.; Chant, S. A. *Environ. Sci. Technol.* **1981**, *15*, 587.
- Robinson, P. J.; Holbrook, K. A. *Unimolecular Reactions*; Wiley-Interscience: London, 1972.
- Masgrau, L.; González-Lafont, A.; Lluch, J. M. *J. Phys. Chem. A* **2002**, *106*, 11760.
- Gaussian 98, Revision A.3: Frisch, M. J.; Trucks, G. W.; Schlegel, H. B.; Scuseria, G. E.; Robb, M. A.; Cheeseman, J. R.; Zakrzewski, V. G.; Montgomery, J. A., Jr.; Stratmann, R. E.; Burant, J. C.; Dapprich, S.; Millam, J. M.; Daniels, A. D.; Kudin, K. N.; Strain, M. C.; Farkas, O.; Tomasi, J.; Barone, V.; Cossi, M.; Cammi, R.; Mennucci, B.; Pomelli, C.; Adamo, C.; Clifford, S.; Ochterski, J.; Petersson, G. A.; Ayala, P. Y.; Cui, Q.; Morokuma, K.; Malick, D. K.; Rabuck, A. D.; Raghavachari, K.; Foresman, J. B.; Cioslowski, J.; Ortiz, J. V.; Stefanov, B. B.; Liu, G.; Liashenko, A.; Piskorz, P.; Komaromi, I.; Gomperts, R.; Martin, R. L.; Fox, D. J.; Keith, T.; Al-Laham, M. A.; Peng, C. Y.; Nanayakkara, A.; Gonzalez, C.; Challacombe, M.; Gill, P. M. W.; Johnson, B.; Chen, W.; Wong, M. W.; Andres, J. L.; Gonzalez, C.; Head-Gordon, M.; Replogle, E. S.; Pople, J. A. Gaussian Inc., Pittsburgh, PA, 1998.
- Frisch, A.; Frisch, M. J. *Gaussian 98 Users Reference*; Gaussian Inc.: Pittsburgh, PA, 1998; p 75.
- Zhang, Q.; Bell, R.; Truong, T. N. *J. Phys. Chem.* **1995**, *99*, 592.
- Durant, J. L. *Chem. Phys. Lett.* **1996**, *256*, 595.
- Braýda, B.; Hiberty, P. C. *J. Phys. Chem. A* **1998**, *102*, 7872.
- Sastry, G. N.; Bally, T.; Hrouda, V.; Carsky, P. *J. Am. Chem. Soc.* **1998**, *120*, 9323.
- Oxgaard, J.; Wiest, O. *J. Phys. Chem. A* **2001**, *105*, 8236.
- Rice, B. M.; Pai, S. V.; Chabalowski, C. F. *J. Phys. Chem. A* **1998**, *102*, 6950.
- Zhang, Y.; Zhao, C. Y.; You, X. Z. *J. Phys. Chem. A* **1997**, *101*, 2879.
- Furuya, K.; Inagaki, Y.; Torii, H.; Furukawa, Y.; Tasumi, M. *J. Phys. Chem. A* **1998**, *102*, 8413.
- Ding, W. J.; Fang, D. C. *J. Org. Chem.* **2001**, *66*, 6673.
- Alvarez-Idaboy, J. R.; Galano, A.; Bravo-Pérez, G.; Ruiz, M. E. *J. Am. Chem. Soc.* **2001**, *123*, 8387.
- Francisco-Márquez, M.; Alvarez-Idaboy, J. R.; Galano, A.; Vivier-Bunge, A. *Phys. Chem. Chem. Phys.* **2003**, *5*, 1392.
- Galano, A.; Alvarez-Idaboy, J. R.; Cruz-Torres, A.; Ruiz-Santoyo, M. E. *Int. J. Chem. Kinet.* **2003**, *35*, 212.
- Galano, A.; Alvarez-Idaboy, J. R.; Bravo-Pérez, G.; Ruiz-Santoyo, M. E. *Phys. Chem. Chem. Phys.* **2002**, *4*, 4648.
- Bravo-Pérez, G.; Alvarez-Idaboy, J. R.; Cruz-Torres, A.; Ruiz-Santoyo, M. E. *J. Phys. Chem. A* **2002**, *106*, 4645.
- Eyring, H. *J. Chem. Phys.* **1935**, *3*, 107.
- Truhlar, D. G.; Hase, W. L.; Hynes, J. T. *J. Phys. Chem.* **1983**, *87*, 2664.
- Duncan, W. T.; Bell, R. L.; Truong, T. N. *J. Comput. Chem.* **1998**, *19*, 1039.
- Eckart, C. *Phys. Rev.* **1930**, *35*, 1303.
- Truong, T. N.; Truhlar, D. G. *J. Chem. Phys.* **1990**, *93*, 1761.
- Truong, T. N. *J. Phys. Chem. B* **1997**, *101*, 2750.
- Truong, T. N.; Duncan, W. T.; Tirtowidjojo, M. *Phys. Chem. Chem. Phys.* **1999**, *1*, 1061.
- Truhlar, D. G.; Isaacson, A. D.; Skodje, R. T.; Garrett, B. C. *J. Phys. Chem.* **1982**, *86*, 2252.
- Rayez, M. T.; Rayez, J. C.; Sawersyn, J. P. *J. Phys. Chem.* **1994**, *98*, 11342.
- Talhaoui, A.; Louis, F.; Devolder, P.; Meriaux, B.; Sawersyn, J. P.; Rayez, M. T.; Rayez, J. C. *J. Phys. Chem.* **1996**, *100*, 13531.
- Chandra, A. K.; Uchimaru, T.; Urata, S.; Sigie, M.; Sekiya, A. *Int. J. Chem. Kinet.* **2003**, *35*, 130.
- Evans, M. G.; Polanyi, M. *Trans. Faraday Soc.* **1938**, *34*, 11.
- Tyndall, G. S.; Orlando, J. J.; Wallington, T. J.; Hurley, M. D.; Goto, M.; Kawasaki, M. *Phys. Chem. Chem. Phys.* **2002**, *4*, 2189.
- Yamada, T.; Taylor, P. H.; Goumri, A.; Marshall, P. J. *Chem. Phys.* **2003**, *119*, 10600.
- Wollenhaupt, M.; Carl, S. A.; Horowitz, A.; Crowley, J. N. *J. Phys. Chem. A* **2000**, *104*, 2695.
- Singleton, D. L.; Cvetanovic, R. J. *J. Am. Chem. Soc.* **1976**, *98*, 6812.
- Pilling, M. J.; Seakins, P. W. *Reaction Kinetics*; Oxford University Press: New York, 1996.
- Laidler, K. J. *Chemical Kinetics*; Harper Collins Publishers: New York, 1987; p 98.
- D'Anna, B.; Bakken, V.; Beukes, J. A.; Nielsen, C. J.; Brudnikb, K.; Jodkowski, J. T. *Phys. Chem. Chem. Phys.* **2003**, *5*, 1790.
- Galano, A.; Alvarez-Idaboy, J. R.; Ruiz-Santoyo, M. E.; Vivier-Bunge, A. *J. Phys. Chem. A* **2002**, *106*, 9520.
- Tomakov, I. V.; Lin, M. C. *J. Phys. Chem. A* **2002**, *106*, 11309.